DINAME 2019 - Proceedings of the XVIII International Symposium on Dynamic Problems of Mechanics,
M.A. Savi, T.G. Ritto and W.M. Bessa (Editors), ABCM, Buzios, RJ, Brazil, March 10th to 15th, 2019

Friction-Induced Vibrations in a Drill-String Experimental Set-Up

Ingrid Pires[1], **Bruno C. Cayres**[1,2], **and Hans I. Weber**[1]

[1] Mechanical Engineering, PUC-Rio, Rua Marquês de São Vicente, 225, Gávea, Rio de Janeiro - RJ, Brazil

[2] CEFET-RJ, Avenida Mario Covas, Santana, Itaguaí - RJ, Brazil

Abstract: Excessive drill-string vibration leads to loss of the drilling process effectiveness and premature damage to the equipment. Due to the drill-string slenderness, torsional vibration is present in most drilling routines, eventually reaching the stick-slip phenomenon. This torsional vibration results from the nonlinear interaction between drill-bits and rocks. Despite the complexity of the bit-rock interaction, the relationship between torque and bit velocity is often treated as dry friction in a slender system. This contribution utilizes experimental and numerical approaches to study dry friction. The experimental approach considers a, so called, drill string experimental set-up, that consists of actuating a slender torsional pendulum where the inertia is subjected to friction with specific particularities. We propose a friction model based on experimental data, and analyze the hysteretic characteristic observed. The experimental results are used to identify the proposed model parameters. Lastly, we compare experimental and numerical results.

Keywords: drill-string vibrations, stick-slip, dry friction, hysteretic cycle

INTRODUCTION

Excessive drill-string vibration leads to loss of the drilling process effectiveness and premature damage to the equipment. What makes the drilling system behavior a challenge to the process enhancement. Several articles in the literature study the drill-string dynamics (Pavlovskaia et al., 2001; Franca, 2004; Jansen, 1991; Vaziri et al., 2018; Ritto et al., 2017).

The drilling system is, basically, composed of a rotary table, drill-string, and drill-bit. The rotary table or top drive is responsible for imposing rotary motion to the system, this motion is transmitted to the bit by the drill string. Besides motion, drill-strings also transmit the required weight to the bit (Bourgoyne Jr et al, 1991). Combining appropriately bit angular velocity and weight on bit is fundamental to induce rock failures. Ideally, the entire drilling system should rotate at a constant speed imposed by the rotary table. Although, due to the drill-string slenderness, torsional vibration is present in most drilling routines, eventually reaching the stick-slip phenomenon.

Stick-slip is a friction-induced limit cycle. In drilling operations, stick-slip happens when friction causes a complete arrest of the drill-bit (stick phase), while the top drive continues to rotate until the stored energy overcomes the friction torque and the bit is released to rotate (slip phase). It is characterized by bit speed high fluctuations that achieve values between zero and up to three times the average top drive speed. These variations are also observed in torque on bit (TOB) and weight on bit (WOB) (Cayres et al., 2018).

Torsional vibration results from the nonlinear bit-rock interaction. Concerning drill-string dynamics, it is essential to study the complex bit-rock interaction characteristics. Literature presents many reports dealing with these interactions (Wiercigroch and Krivtsov, 2001; Patil and Teodoriu, 2013; Hong et al., 2016). Despite the complexity of the bit-rock interaction, the relationship between torque and bit velocity is often treated as dry friction in a slender system. Tribological experiments have observed the existence of hysteresis phenomenon, that is the friction force during tangential acceleration is higher than during deceleration (Leine, 2004). Some recent papers as "Real et al. (2018)" analyze the hysteretic rock-bit interactions characteristic, observed in down-hole field measurements.

This contribution utilizes experimental and numerical approaches to study dry friction. The experimental approach considers a, so called, drill string experimental set-up, that consists of actuating a slender torsional pendulum where the inertia is subjected to friction with specific particularities. In this paper, we propose a hysteretic friction model based on experimental studies and well-known friction characteristics. Lastly, we compare experimental and numerical results.

TEST RIG DESCRIPTION

To reproduce the torsional vibrations experienced by real drill-strings, the experimental apparatus used in this analysis was designed and built at Pontifícia Universidade Católica do Rio de Janeiro. Since torsional vibrations are the subject of interest, the rig was designed to isolate the torsional from lateral and axial modes of vibration (Cayres, 2013).

Figure 1 presents the test rig, which is composed of two discs, D1 and D2, and a DC-motor inertia, D3. The three inertia are connected by a low-stiffness shaft, that transmits the rotation from the DC-motor to the discs. To obtain all state variables of the system, the rig is equipped with sensors and transducers.

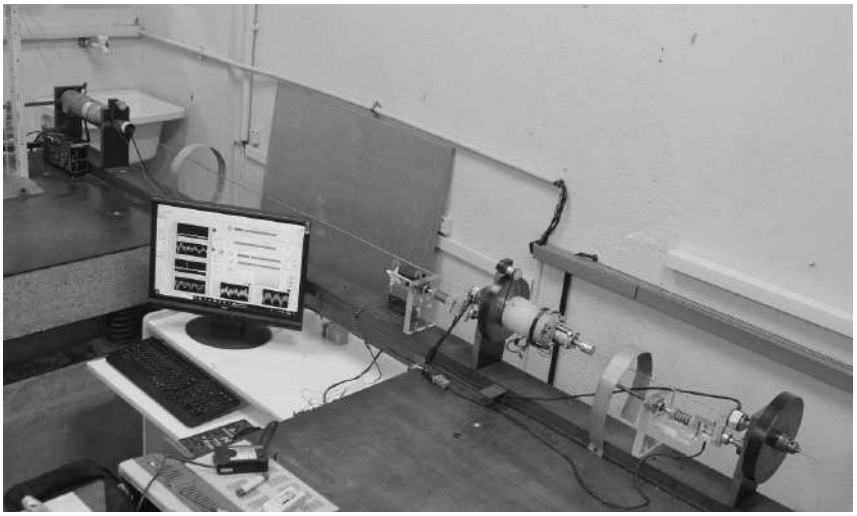

Figure 1: Drill-string experimental set-up (Cayres et al., 2018).

There are two brake devices in the system to induce friction torque, placed in discs D1 and D2. The dry contact between the brake device pin and the disc produces friction torque, leading the system to experience torsional vibrations and stick-slip. The normal force produced by the pin and disc contact is acquired by load cells. In this study, we are restricting our analysis to the reduced system composed of the DC-motor, the disc D2 and the shaft that connects them. Therefore, we are only considering the friction torque on the disc D2. Figure 2 shows the brake device placed on disc D2.

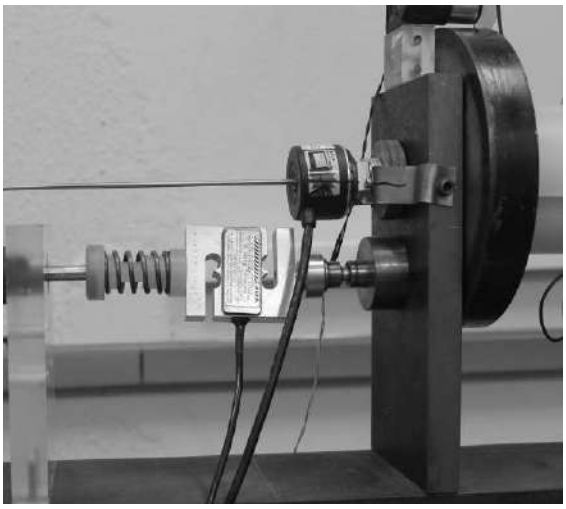

Figure 2: Brake device and measure components placed in disc D2.

DYNAMIC MODEL

This section introduces an experimental drill-string set-up dynamic model. Figure 3 presents a schematic system representation. To model the test-rig response, the system was divided into mechanical and electrical subsystems.

The mechanical subsystem is composed of discs D2, and the shaft connecting it to the DC-motor. Disc D2 have a moment of inertia J_2. The shaft linear stiffness is denoted by k_2, and the linear damping is denoted by d_2. Although simple, torsional pendulum model can describe stick-slip phenomenon very well, by using this model the system may be mathematically expressed as

$$\begin{aligned} J_2\ddot{\theta}_2 + d_2(\dot{\theta}_2 - \dot{\theta}_3) + k_2(\theta_2 - \theta_3) &= -T_{f2}, \\ d_2(\dot{\theta}_3 - \dot{\theta}_2) + k_2(\theta_3 - \theta_2) &= \tau_s, \end{aligned} \tag{1}$$

where θ, $\dot{\theta}$, and $\ddot{\theta}$ are angular displacement, angular velocity and angular acceleration, respectively. In Eq. (1), τ_s is the

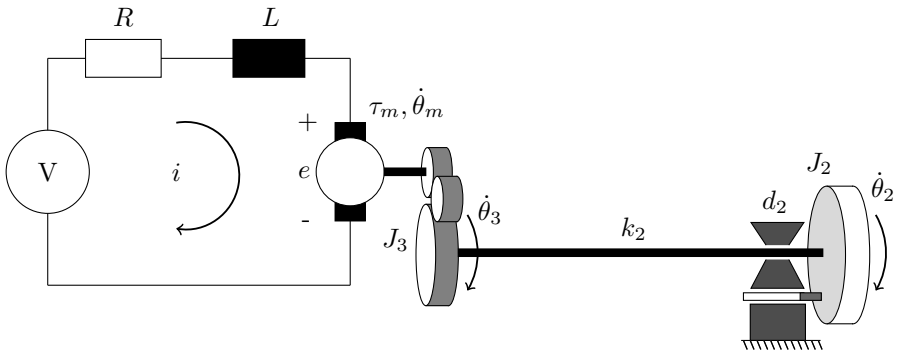

Figure 3: Schematic representation of the drill-string set-up (adapted from Pereira et al., 2018)

torque given to the system, while T_{f2} is the resistive friction torque on disc D2.

The electric subsystem is modeled as a voltage source connected in series with a resistor and an inductor, providing torque τ_m. The angular velocity $\dot{\theta_m}$ imposed by τ_m is eight times greater than the angular velocity $\dot{\theta}_3$ transmitted to the mechanical subsystem due to the transmission factor $\eta = 8:1$.

Mathematically, the electric subsystem may be expressed as

$$\begin{aligned} L\frac{di}{dt} &= V - Ri - K_E\dot{\theta}_m, \\ \tau_m &= K_T i - C_m\dot{\theta}_m - T_f - J_m\ddot{\theta}_m, \end{aligned} \tag{2}$$

where i denotes DC-motor electric current. L and R are the armature inductance and resistance, respectively. The angular velocity $\dot{\theta_m}$ is the velocity of the DC-motor inertia, J_m. C_m is the speed regulation; K_T, the constant motor torque; K_E, the voltage constant; and T_f, the internal friction torque.

The input voltage is denoted by V, and is modelled by

$$V = \kappa_p(\omega_{ref} - \dot{\theta}_3) + \kappa_i \int_0^t (\omega_{ref} - \dot{\theta}_3)dt, \tag{3}$$

where κ_p and κ_i are proportional constant and integral constant, respectively, and ω_{ref} is the reference velocity of the system. The relations between the mechanical and electrical subsystems are giving by

$$\begin{aligned} \tau_s &= \eta\,\tau_m, \\ \dot{\theta_m} &= \eta\,\dot{\theta}_3. \end{aligned} \tag{4}$$

The mechanical and electrical systems coupling results in the following set of equations

$$\begin{aligned} J_2\ddot{\theta}_2 + d_2(\dot{\theta}_2 - \dot{\theta}_3) + k_2(\theta_2 - \theta_3) &= -T_{f2}, \\ d_2(\dot{\theta}_3 - \dot{\theta}_2) + k_2(\theta_3 - \theta_2) &= \eta(K_T i - C_m\eta\,\dot{\theta}_3 - T_f - J_m\eta\,\ddot{\theta}_3, \\ L\frac{di}{dt} + Ri + K_E\eta\,\dot{\theta}_3 &= V. \end{aligned} \tag{5}$$

ADOPTED DRY FRICTION MODEL

The friction force is the resistance to the relative motion of two contact surfaces. Coulomb friction model is often used to model the dry friction force (Leine, 2004). Although simple, this classical linear model does not explain all dynamical characteristics of mechanical systems with friction. Thus, nonlinear models are used for better approximations of real systems. Besides nonlinearities, some studies argue that there are lower values of friction force for decreasing velocities than increasing velocities (Leine, 2004).

Our experimental results not only present the nonlinear friction characteristics but also hysteretic friction characteristics. According to Wojewoda (2007), there are three different types of hysteretic effects accompanying frictional processes: one that can appear during sticking, one that can appear during the switch between stick and slip phases, and one that can appear during oscillations with pure sliding. We observed the presence of the last effect in our test-rig results.

The experimental results and previous studies motivated us to propose a different dry friction model. The idea was to formulate a simple model to be implemented in numerical calculations able to reproduce the experimental friction phenomena. Its mathematical description has the following form

$$T_{f2} = \begin{cases} a\dot{\theta}_2 & \text{if } \left|\dot{\theta}_2\right| \leq \omega_s, \\ p_{00} + p_{10}\dot{\theta}_2 + p_{01}\ddot{\theta}_2 + p_{20}\dot{\theta}_2^2 + p_{11}\dot{\theta}_2\ddot{\theta}_2 + p_{02}\ddot{\theta}_2^2 & \text{if } \left|\dot{\theta}_2\right| > \omega_s, \ddot{\theta}_2 > 0, \\ n_{00} + n_{10}\dot{\theta}_2 + n_{01}\ddot{\theta}_2 + n_{20}\dot{\theta}_2^2 + n_{11}\dot{\theta}_2\ddot{\theta}_2 + n_{02}\ddot{\theta}_2^2 & \text{if } \left|\dot{\theta}_2\right| > 10^{-3}, \ddot{\theta}_2 < 0, \end{cases} \tag{6}$$

where $\omega_s = 10^{-3}$.

We used the experimental results to identify the polynomial coefficients. This model considers the friction torque as a function of relative velocity and acceleration. Moreover, we use one linear function to describe the resistive friction torque during the "stick" phase and two 2^{nd} order functions, during the "slip" phase.

The choice for representing the torque as a function of both velocity and accelerations is explained by the different characteristics of the experimental curves for acceleration and decelaration. In other words, the friction torque decreases with the increase in velocity as a function of velocity and acceleration and increases with the decrease in velocity as another function of the same variables. The different curves are clear in the performed test and are presented in the next section.

Although one polynomial function of velocity and acceleration is enough to reproduce the system dynamics, we are also interested in reproducing the double loop aspect of the experimental toque. That's the reason we use two polynomial functions.

EXPERIMENTAL AND NUMERICAL STUDIES

To propose the friction model, we performed the tests for a normal force/reference velocity combination where stick-slip is fully developed and the disc D2 sticks, and where the torque-velocity hysteretic characteristic is clear. We used a reference velocity of 5.76 rad/s (55 rpm), and a normal force, N2, on disc D2 equal to 35 N.

In our experimental studies, we determined the friction force indirectly on the basis of a simplified rig mathematical model given by Eq. (1). According to Eq. (1), an indirect rig friction force estimation requires three signals and three frictional system parameters. The required signals are the relative displacement, $\theta_2 - \theta_3$, measured directly by the encoders, and the relative velocity, $\dot{\theta}_2 - \dot{\theta}_3$, and the acceleration on disc D2, $\ddot{\theta}_2$, differentiated from the displacement signals. The required parameters of the rig were determined from experimental investigations.

Figure 4 shows the experimental results for this parameter combination. In figure 4a, we can see the oscillation of the DC motor and disc D2 angular speeds. In figure 4b, the torque variation is presented. The existence of the stick-slip phenomenon is evident during the test.

Figure 5a plots the friction torque versus disc D2 speed. This graph is often used to characterize bit-rock interaction in drill-strings torsional vibrations. The Stribeck effect, that is the decrease in friction torque with the increase in velocity, is present. We can also identify the hysteresis effect, i.e. torque decreases when bit speed increase in a different path then it increases while bit speed decreases. Once we are arguing that friction torque not only varies with the relative velocity but also with the relative acceleration, figure 5b plots the torque versus disc D2 acceleration. At last, figure 5c plots the disc D2 acceleration versus its velocity.

To better analyze how the resistive friction torque imposed to disc D2, we adopted a tridimensional representation. The tridimensional graph is in figure 6 and shows how friction varies with both disc D2 velocity and acceleration.

In the numerical simulation, the dynamical model given by Eq. 5 and the friction characteristics presented in Eq. 6 were used. Tables 1 and 2 present the parameters values used in the simulation.

Table 1: Test rig mechanical parameters.

Parameter	Description	Value	Unit
J_2	D_2 moment of inertia	0.0149	kgm^2
J_3	DC-motor moment of inertia	0.0237	kgm^2
k_2	stiffness between D_2 and DC-motor	0.3659	Nm/rad
d_2	damping between D_2 and DC-motor	0.0167	Nms/rad

Figure 7 present the numerical simulations and the experimental results.

As we can see from figure 7, the numerical simulations correspond well to the experimental results. In both results,

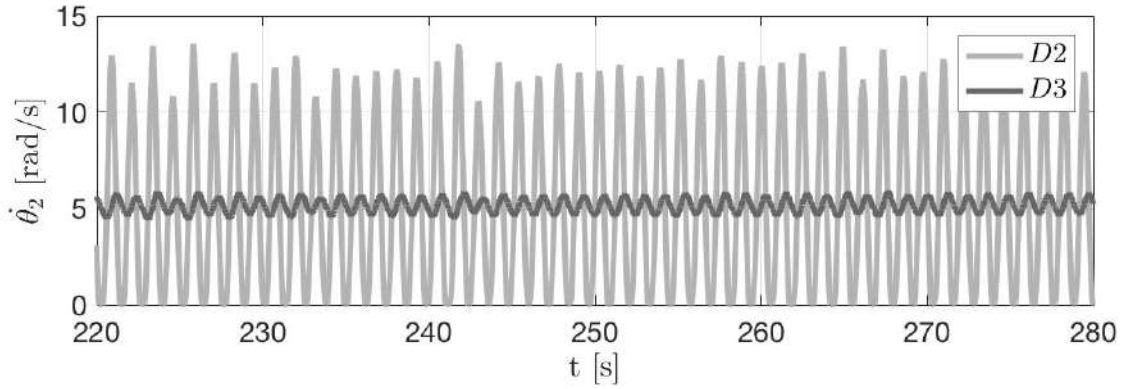

(a) Experimental velocity of discs D2 and D3.

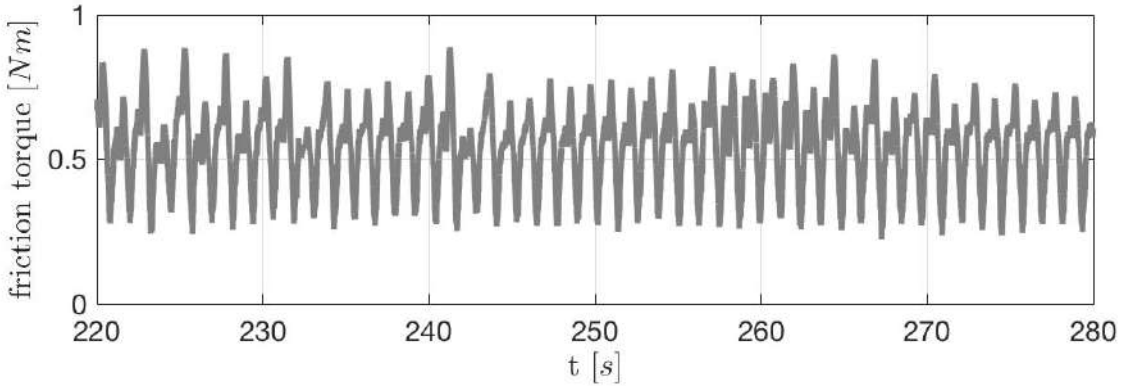

(b) Experimental friction torque on disc D2.

Figure 4: Test rig angular velocity of disc D2(top) and torque on disc D2(bottom) for 5.76 rad/s (55 rpm) and N2 = 35.0 N.

Table 2: DC-motor electrical parameters.

Parameter	Description	Value	Unit
L	armature inductance	$8.437(10^{-4})$	H
R	armature resistance	0.33	Ω
K_T	torque constant	0.126	Nm/A
K_E	voltage constant	0.0602	$V/(rad/s)$
T_f	friction torque	0.1196	Nm
C_m	speed regulation constant	$1.784(10^{-4})$	$Nm/(rad/s)$
κ_p	proportional constant	2.800	-
κ_i	DC-motor moment of inertia	3.500	-

it is possible to notice that the velocity of disc D2 is always positive, as expected from prior experience. The system experimental frequency of oscillation was found to be 0.83 Hz and the calculated numerical frequency oscillation was 0.84 Hz. Despite the agreement of the results, there is a difference between the amplitudes of disc D2 velocity oscillations. While the maximum experimental amplitude of oscillation is equal to 13.55, the amplitude obtained numerically is equal to 14.

DISCUSSION

This research effort intends to propose a friction model based on the data obtained from the aforementioned test. The previous section presents the system response for a reference velocity of 55RPM and a normal force of 35N. We used the system response to analyze the dynamical behavior of the system. From the state variables values attained by the performances, we propose a friction model that takes an account of the hysteretic characteristic of the dry friction noticed in the experimental results. Subsequently, we justify the proposed friction model numerically, applying the lumped

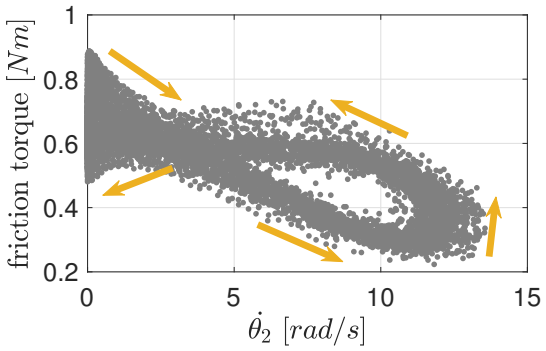

(a) Torque vesrus velocity.

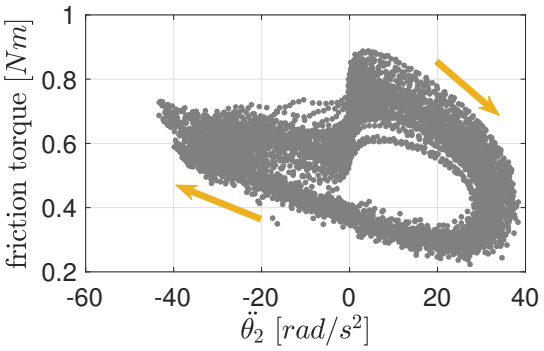

(b) Torque vesrus acceleration.

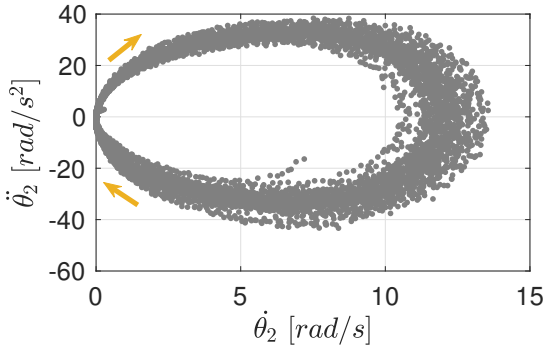

(c) Acceleration vesrus velocity

Figure 5: Experimental results for a nominal velocity of 55RPM and a normal force of 35N.

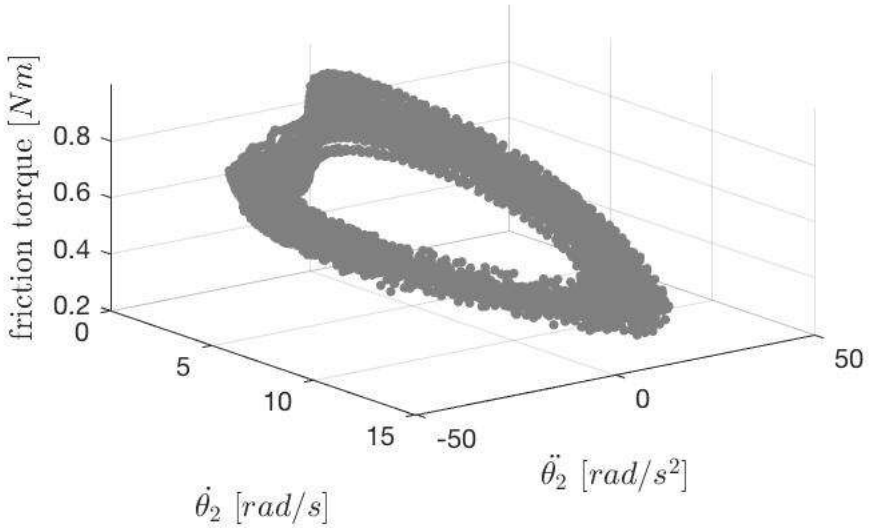

Figure 6: Experimental friction torque tridimensional curve for a nominal velocity of 55RPM and a normal force of 35N.

parameters method.

The comparisons between numerical and experimental data (figure 7) confirm that the proposed dry friction model is a good approximation of the observed frictional phenomena. We also observe that the amplitudes of oscillation differ, but we may well represent the oscillation frequency.

As a continuation of this work, the authors aim to improve the friction model in order to reproduce with greater precision the dynamics of the experimental system.

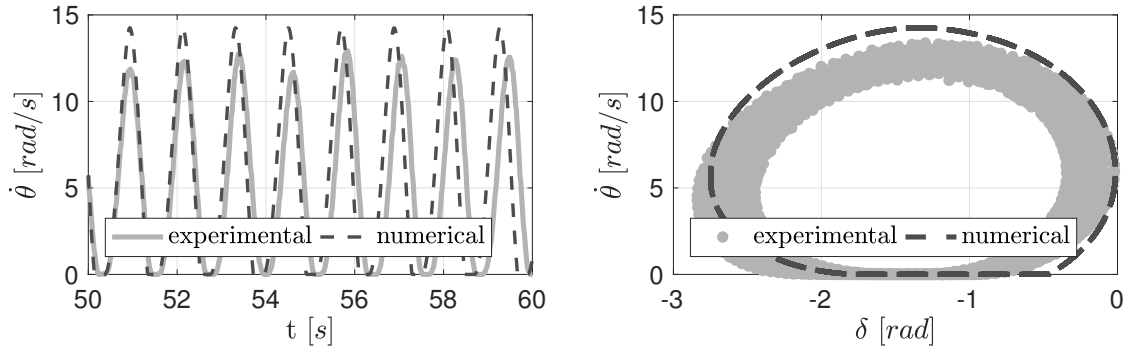

(a) Angular velocity

(b) Phase portrait

Figure 7: (a) Experimental (continuous) and numerical (dashed) angular velocity, and (b) experimental (dotted) and numerical (dashed) phase portraits of disc D1 for a nominal velocity of 55RPM and a normal force of 35N.

ACKNOWLEDGMENTS

The authors acknowledge the support given by CAPES.

REFERENCES

Bourgoyne JR., A.T.; Millheim, K.K.; Chenevert, M.E.; Young JR., F.S., 1991, "Applied drilling engineering". SPE Textbook Series, Dallas, TX, Vol. 2.

Cayres, B.C., Fonseca, C.A., Sampaio, G., Weber, H.I., 2018, "Analysis of a drill-string experimental set-up with dry friction-induced torsional vibration", IFToMM International Conference on Rotordynamics, Vol. 3.

Cayres, B., 2013, "Numerical and experimental analysis of nonlinear torsional dynamics ofa drilling system". M.Sc. Thesis, Pontíficia Universidade Católica do Rio de Janeiro, Rio de Janeiro, Brazil.

Franca, L.F.P., 2004, "Self-Excited Percussive-Rotary Drilling in Hard Rocks." D.Sc. Thesis, Pontificia Universidade Catolica do Rio de Janeiro, Rio de Janeiro, Brazil.

Hong L., Girsang, P.I.,Dhupia, J. S, 2016, "Identification and control of stick?slip vibrations using Kalman estimator in oil-well drill strings", Journal of Petroleum Science and Engineering, Vol. 140, pp. 119-127.

Jansen, J.D., 1991, "Non-linear rotor dynamics as applied to oilwell drillstring vibrations", Journal of Sound and Vibration, Vol. 147, pp. 115-135.

Leine, R.I., Nijmeijer, H., 2004, "Dynamics and Bifurcations of Non-Smooth Mechanical Systems". Lecture Notes in Applied and Computational Mechanics Vol. 18, Netherlands.

Patil, P., Teodoriu, C., 2013, "Analysis of bit rock interaction during stick slip vibration using PDC cuttting force model", DGMK German Society for Petroleum and Coal Science and Technology, Celle, Germany.

Pavlovskaia, E., Wiercigroch, M., Grebogi, C., 2001, "Modeling of an impact system with a drift", Physical Review, Vol. 64.

Pereira, L.D., Cayres, B.C., Weber, H.I., 2018, "Numerical application of a stick-slip control and experimental analysis using a test rig", MATEC Web of Conferences, Vol. 148.

Real, F.F., Batou, A., Ritto, T.G., Desceliers, C., Aguiar, R.R., 2018, "Hysteretic bit/rock interaction model to analyze the torsional dynamics of a drill string", Mechanical Systems and Signal Processing, Vol. 111, pp. 222-233.

Ritto, T.G., Aguiar, R.R., Hbaieb, S., 2017 "Validation of a drill string dynamical model and torsional stability", Meccanica, Vol. 52, pp. 2959-2967.

Vaziri, V., Kapitaniak, M., Wiercigroch, M., 2018 "Suppression of drill-string stick?slip vibration by sliding mode control: Numerical and experimental studies", European Journal of Applied Mathematics, pp 1-21.

Wiercigroch, M., Krivtsov, A., 2001 "Frictional chatter in orthogonal metal cutting", Philosophical Transactions of the Royal Society of London A: Mathematical, Physical and Engineering Sciences, Vol. 359, pp. 713-738.

Wojewoda, J., Stefanski, A., Wiercigroch, M., Kapitaniak, T., 2008 "Hysteretic effects of dry friction: modelling and experimental studies", Philosophical Transactions of the Royal Society of London A: Mathematical, Physical and Engineering Sciences, Vol. 366, pp. 747-765.

RESPONSIBILITY NOTICE

The author(s) is (are) the only responsible for the printed material included in this paper.